J. of Supercritical Fluids 125 (2017) 1–11

Contents lists available at ScienceDirect

The Journal of Supercritical Fluids

journal homepage: www.elsevier.com/locate/supflu

Experimental measurement and modeling of quinizarin solubility in pressurized hot water

M.F. Barrera Vázquez[a,b,*], N.A. Gañan[a,b], L.R. Comini[c], R.E. Martini[a,b], S.B. Bottini[d], A.E. Andreatta[a,e]

[a] IDTQ – Grupo Vinculado PLAPIQUI – CONICET, Córdoba, Argentina
[b] UNC, Facultad de Ciencias Exactas Físicas y Naturales, Av. Vélez Sarsfield 1611, CU, Córdoba, Argentina
[c] Farmacognosia, Departamento de Farmacia, Facultad de Ciencias Químicas, Universidad Nacional de Córdoba – IMBIV, CONICET, Ciudad Universitaria, Córdoba, Argentina
[d] PLAPIQUI (UNS-CONICET), Cno. La Carrindanga Km 7, Bahía Blanca, Argentina
[e] UTN, Facultad Regional San Francisco, Av de la Universidad 501, San Francisco, Córdoba, Argentina

ARTICLE INFO

Article history:
Received 1 August 2016
Received in revised form
28 December 2016
Accepted 29 December 2016
Available online 31 December 2016

Keywords:
Anthraquinones
Pressurized hot water
Association equation of state
Phase equilibria

ABSTRACT

In the field of natural products, anthraquinones are an important category of secondary metabolites present in various vegetable species. They are highly bioactive compounds, potentially useful for therapeutic applications, as antiviral, anti-bacterial and anti-cancer agents. Extraction processes using pressurized hot water offer an environmentally friendly alternative to traditional extraction and purification methods applied to anthraquinone-containing plants. Knowledge on high-pressure phase equilibria of anthraquinone + solvent mixtures is required to evaluate the potentiality of these processes. The need is for both, experimental data and thermodynamic models that are able to predict phase boundaries at different process conditions. In this work, the solubility of 1,4-dihydroxy-9,10-anthraquinone (quinizarin) in pressurized hot water has been measured, using a simple and reliable dynamic method. For the binary quinizarin + H_2O, the measurements were performed at (333, 353, 373, 393, 413, 443, 463) K and pressures of (30, 60 and 90) bar. The group-contribution with association equation of state (GCA-EOS), with the definition of a cyclic ketone functional group (CyC=O) was used to calculate solid-liquid equilibria of binary mixtures of anthraquinones with pressurized hot water. This model was able to give a good representation of the solubility behaviour of quinizarin in water.

1. Introduction

Throughout history, natural products have been a rich source of compounds with many applications in the field of medicine and in the pharmaceutical industry. In microbiology, particularly, several plant-derived compounds have been studied with this aim, including alkaloids, flavonoids, tannins, quinones, essential oils and other secondary metabolites [1]. Among them, anthraquinones (AQs), the most numerous group of quinones present in the vegetable kingdom [2], constitute an important group of secondary metabolites having potential therapeutic applications. AQs have exhibited significant biological activities, such as antibacterial, antifungal and antiviral effects [3–7].

Natural AQs can be divided into two groups, according to the biosynthetic pathway that originated them: (a) via acetate – malonate and (b) shikimic acid pathway-*o*-succinilbenzoic acid and mevalonate. These two kinds of AQs have different substitution patterns, and this is related to the therapeutic effects exhibited [8].

Quinizarin (Fig. 1a) is the 1,4-dihydroxy-9,10-anthraquinone synthesized via the shikimic acid – *o*-succinilbenzoic acid and mevalonate pathway, with substitution in the C ring. It has been isolated and identified from different plant species such as *Rubia Tinctorium* [9] and *Cassia tora* seeds [10]. This AQ has important potential applications in the field of medicine, demonstrating inhibitory effects against human intestinal bacteria (*Clostridium perfringens* and *Sthaphylococcus aureus*). In addition, quinizarin exhibits inhibitory effects in the Aflatoxin B1 biotransformation to the corresponding 8,9-epoxides, which are responsible of the toxic and carcinogenic effects of aflatoxins, secondary metabolites produced primarily by the *Aspergillus flavus* and *Aspergillus parasiticus* fungi [11,12].

* Corresponding author at: UNC, Facultad de Ciencias Exactas Físicas y Naturales, Av. Vélez Sarsfield 1611, CU, Córdoba, Argentina.
E-mail address: mfbarreravazquez@plapiqui.edu.ar (M.F. Barrera Vázquez).

http://dx.doi.org/10.1016/j.supflu.2016.12.020
0896-8446/

Nomenclature

List of symbols

A^{assoc}	Helmholtz energy term describing association part
A^{att}	Helmholtz energy term describing attractive part
A^{fv}	Helmholtz energy term describing free volume part
d_{ci}	Hard sphere diameter of the component i (cm mol^{-1})
d_i	Diameter of the component i (cm mol^{-1})
g_{ij}	Attraction energy parameter for interactions between groups *i* and *j* (atm.cm^6 mol^{-1})
k_B	Boltzman constant
k_{ij}, k_{ji}	Binary interaction parameters
M_i	Number of associating sites assigned to group *i*
n^*_j	Number of moles of associating group *j*
NC	Number of components in the mixture
NGA	Number of associating groups
N^{set}	Number of experimental data sets
N^{exp}	Number of experimental data points
n_i	Number of moles of component *i*
P	Pressure
P_c	Xritical pressure
q	Surface-area segments per mole
$\tilde{q}$	Total number of surface segments
q_j	Number of surface segments assigned to group *j*
R	Ideal gas constant
s	Solubilities (mg/ml)
SD	Standard deviation
T	Temperature (*K*)
T_b	Boiling temperature
T_c	Critical temperature
T_{ci}	Critical temperature of component *i* (*K*)
T_f	Melting temperature
T_r	Reduced temperature
V	Volume (cm^3)
$X^{(k,i)}$	Fraction of not bonded site k of group *i*
x_i	Mole fraction in liquid phase of component *i*
y_i	Mole fraction in vapor phase of component *i*
y	Solublities in mole fraction
z	Number of nearest neighbors to any segment

Greek letters

α_{ij} α_{ji}	Non-randomness parameters
$\Delta^{(k,i,l,j)}$	Association strength between site *k* of group *i* and site *l* of group *j* (cm^3 mol^{-1})
ΔH_f	Enthalpy of fusion
$\varepsilon^{(k,i,l,j)}$	Association energy between site *k* of group *i* and site *l* of group *j* (K)
φ	Fugacity coefficient
$\kappa^{(k,i,l,j)}$	Association volume between site *k* of group *i* and site *l* of group *j* (cm^3 mol^{-1})
ρ	Density (mol cm^{-3})
$\rho_j{}^*$	Molar density of the associating group *j* (mol.cm^{-3})
ν_{ij}	Number of group *j* in molecule *i*
$\nu_{assoc}{}^{(i,m)}$	Number of associating groups *i* present in molecule *m*
θj	Surface fraction of group j

Traditionally, AQs are obtained from vegetable matrices by Soxhlet liquid-solid extraction using organic solvents [13–16]. For example, quinizarin is obtained from the *Cassia tora* seeds by means of maceration and successive application of column chromatography techniques (silica gel, Sephadex LH-20, Polyclar AT and cellulose) using methanol, hexane, chloroform, ethyl acetate, butanol and water as extraction solvents, and different proportions of chloroform/acetone/methanol as purification solvents [10]. These conventional techniques require high residence times, use large quantities of solvent, present low selectivity and have a negative impact on the environment and human health [17,18]. In this sense, pressurized hot water extraction (PHWE) is a very interesting alternative for the extraction and purification of these substances, because it is an environmentally friendly separation technique carried out at high temperatures (usually from 373 to 643 K) and under a pressure sufficiently high (usually from 10 to 221 bar) to maintain water in the liquid state [19–21].

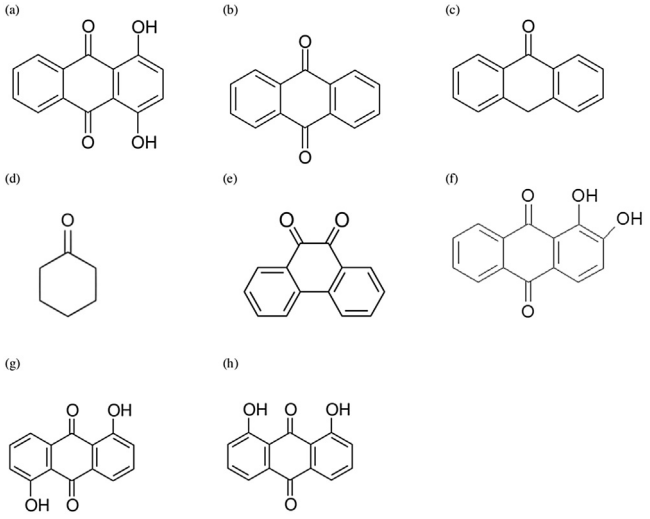

Fig. 1. Chemical structure of cyclic ketones compounds studied in this work. (a) 1,4-dihydroxy-9,10-anthraquinone (quinizarin), (b) 9,10-anthraquinone, (c) anthrone, (d) cyclohexanone, (e) 9,10-phenanthrenequinone, (f) 1,2-dihydroxy –9,10-anthraquinone, (g) 1,5-dihydroxy-9,10-anthraquinone, (h) 1,8-dihydroxy –9,10-anthraquinone.

In a previous work [22] it was demonstrated that PHWE is a potential alternative method for extracting AQs from *Heterophyllaea pustulata*. The results showed a yield of AQs in optimal conditions almost six times the yield obtained by traditional Soxhlet extraction using solvents of increasing polarity [23]. However with the extraction assisted ultrasonics (EAU) + extraction assisted microwave (EAM) combination using benzene and ethyl acetate solvents, a good yield of AQs is obtained, but the solvents used for the extraction are hazardous to health [23]. From this point of view, PHWE technology is a good alternative, using water as a solvent. Similar results can be found in the literature for the extraction of AQs from the roots of *Morinda citrifolia* [24–26].

AQs have melting points above 523 K. Even though the solubility of AQs in water is very low at room temperature, the use of PHWE is attractive because the solubility of solid solutes increases as the temperature becomes closer to their melting points. Karásek et al. [27] found that the mole fraction of 9,10-anthraquinone in pressurized hot water increases over 400 times from 313 K to 433 K. In addition, these authors used the experimental solubilities to calculate the activity coefficients of various oxygenated aromatic solutes in aqueous solutions at saturation. Pongnaravane et al. [25] used a static and a dynamic method to measure the solubility of alizarin in hot water. They found that the mole fraction of alizarin increased about 6 times in the temperature range between 398 K and 473 K. Additionally, these authors use a mathematical model proposed by Miller et al. [28], in which developed an approximation model for the mole fraction solubility of polycyclic aromatic hydrocarbons and pesticides in subcritical water. The approximation for the model assumes that the Gibbs function for the solution does not

Table 1
Chemicals used in the experimental work.

Chemical name	CAS number	Source	Purity*
Methanol	67–56-1	Cicarelli, Argentina	99
Quinizarin	81–64-1	Sigma Aldrich, USA	≥96

* No previous purification was performed.

change over the temperature range and there is no absorption of water by the solute.

Thermodynamic models based on cubic equations of state with different mixing rules have been applied with success to calculate the solubility of solid solutes in pressurized carbon dioxide [29–31]. Yet, extrapolation of these models to temperatures or pressures outside the regression window is not guaranteed, as binary interaction parameters obtained from regression of solid-gas equilibria data do not seem to follow any general trend [31]. Furthermore, extrapolation to solutes for which no experimental data are available is not possible. In this sense, group contribution models have an advantage over molecular models: a large number of compounds and mixtures can be represented with a reduced number of functional groups, but unfortunately it does not distinguish the position isomers.

In this work, the solubility of quinizarin in pressurized hot water was measured, using a simple and reliable dynamic method, at temperatures of (333, 353, 373, 393, 413 and 443) K and pressures of (30, 60 and 90) bar. Solid-liquid equilibria of binary mixtures of AQs with pressurized hot water, was calculated using the group-contribution with association equation of state GCA-EOS [32]. For this purpose, a cyclic ketone functional group (CyC=O) was defined. The parameters of this new functional group were determined by fitting experimental data of pure compounds and binary systems.

2. Materials and methods

2.1. Chemicals

The water used in the experimental solubility measurements is bydistilled, obtained in a water distiller (FM4 Figmay, Argentina). The degassing of oxygen dissolved in the water was removed by the application of ultrasound (TB02TACF, TESTLAB SRL). Table 1 shows CAS number, purity and supplier of the chemicals used in the experimental.

2.2. Measurement of quinizarin solubility

The experimental solubility measurements were carried out in a high-pressure device designed and built in our group. It consists of a stainless steel high-pressure extractor cell with 10 ml internal volume, a HPLC pump (Waters 501, Dickinson, Texas, USA) having a maximum flow rate of 10 ml/min, a coiled preheater and a downstream back pressure regulator (BPR). The extraction cell is equipped with a heating system consisting of aluminum heating jackets with two electrical resistances, connected to a temperature regulator. The cell is installed within a thermally insulated box, to facilitate isothermal conditions during operation. The pressure in the extractor is measured with a pressure gauge (Dynisco Dynipack 16, Franklin, Massachusetts, USA). The experimental apparatus is completed with stainless steel connecting lines and accessories. Fig. 2 shows a diagram of the experimental setup. More details about the equipment and the operating process can be found in Barrera Vázquez et al. [23].

To begin the solubility measurements, 0.5 g of quinizarin, embedded on glass beads (35–60 mesh), are loaded into the cell. After closing the system, the operating temperatures of the preheater and cell are set. The BPR is used to set the pressure at the

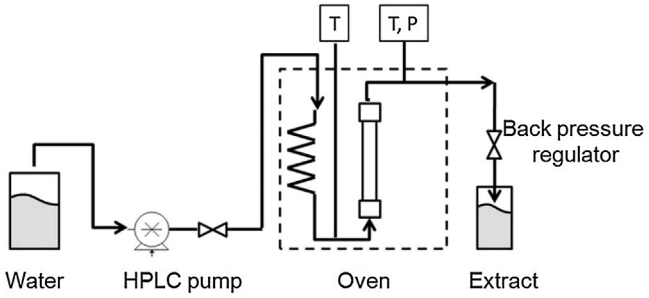

Fig. 2. Schematic diagram of high pressure apparatus.

operating value. The quinizarin solubility has been measured at (333, 353, 373, 393, 413 and 443) K and (30, 60 and 90) bar with an uncertainty of ±0.5 K and ±1 bar respectively. The water flow rate used in these experiments was 0.75 ml/min (0.75 g/ml). This flow rate was slow enough to ensure equilibrium conditions within the cell and it was selected based in preliminary studies. This procedure was performed for triplicate for each temperature and pressure condition tested. Immediately upon leaving the equipment, 1 ml of sample was diluted in 10 ml of methanol for further analysis by UV–vis spectrophotometry, maintaining a constant temperature of 298 K.

The concentrations of quinizarin were determined by spectrophotometry by measuring the absorbance (at 480.18 nm) of each solution afore mentioned (1 ml of sample in 10 ml of methanol) at each tested condition. The measurements were carried out using the Lambda 25 UV–vis spectrophotometer (Perkin Elmer, USA).

Quinizarin was quantified (mg/ml) in each sample obtained using the external calibration method where solutions of quinizarin between 0.01 and 0.6 mg/ml were prepared in H_2O:MeOH (1:10 v/v) at 298 K by triplicate.

Calibration curves were obtained by graphing the absorbance as a function of quinizarin concentration. The curve constructed was linear (correlation coefficients = 0.9972). Using the calibration curve, the concentration of quinizarin in each sample obtained to the different conditions tested was calculated using the following linear equation Y = 44.41 X- 0.0323, where Y is the absorbance and X the concentration of quinizarin, whose deviation from the origin of Cartesian axes may be due to various factors, such as instrumental deviation. The obtained results were used to calculate the quinizarin solubility in pressurized hot water taking into account the dilution made with methanol. All solution (both those obtained during the experimental procedure and those used to make the calibration curve) were protect away from light using brown glass flask.

2.3. Solid-liquid equilibria modelling

The group contribution equation of state (GC-EOS) was originally developed by Skjold-Jørgensen [33,34] to calculate vapor–liquid equilibria of non-ideal mixtures of low to medium molecular weight compounds, up to pressures of 250–300 bar. Espinosa et al. [35] extended the application of the model to low-volatile, high-molecular weight compounds. Using a unique set of parameters, a satisfactory correlation and prediction of vapor–liquid and liquid–liquid equilibria of mixtures of supercritical fluids with natural oils and derivatives were achieved [36].

The basis of the GC-EOS equation is a generalized van der Waals partition function combined with the local composition principle and a group-contribution approach. The required parameters of the model are the temperature-dependent pure-group energy parameter (g_{ii}) and the binary and non-random interaction parameters between functional groups (k_{ij} and α_{ij}). The Carnahan-Starling

repulsive term contains a molecular parameter (the critical hard sphere diameter, d_c) that is modeled assuming a hard sphere behavior for the molecules. Each substance i is characterized by its hard sphere diameter d_i, which is assumed to be temperature dependent.

For liquid solvents, d_{ci} is fitted to pure component vapor pressure data, whereas for gases and supercritical fluids, the d_{ci} value is calculated from critical properties (see Appendix A).

Gros et al. [32] extended the application of the GC-EOS equation to associating systems, by adding a third term, based on Wertheim's theory of fluids with highly directed attractive forces, to take into account association effects (the so called GC Associating EOS). The Appendix A contains a brief explanation of the GCA-EOS equation. Gros et al. [32], applied of the model to alcohols, water, gases, and their mixtures, using a single self-associative hydroxyl (OH) group. Later, the GCA-EOS has been successfully employed to represent phase equilibria in mixtures containing water, alcohols, carboxylic acids, esters, ketones, cyclic compounds, aromatic hydrocarbons and alkanes [37–45].

When the equilibrium involves a solid phase, is not possible to use a conventional cubic equation of state to calculate directly the fugacity in that phase, because they do not represent adequately the properties of a solid phase. However, it is possible to calculate the fugacity of the solid solute, relating it to the "hypothetical" vapor or liquid sub-cooled fugacity at the solid temperature [46].

In the first case, the fugacity of the pure solid solute at temperature T and pressure P, $f^S(T,P)$ is calculated from the fugacity of the vapor in equilibrium with the solid at temperature T and the corresponding sublimation pressure P^{sub}, corrected with the Poynting expression to take account of the change of fugacity of a condensed phase with pressure, according to Eq. (1):

$$f_i^S(T,P) = \phi_i^V(T,P_i^{sub})P_i^{sub}\exp\left[\frac{V_i^S}{RT}\left(P-P_i^{sub}\right)\right] \tag{1}$$

In this equation ϕ_i^V is the fugacity of the pure solid solute in the vapor phase at temperature T and sublimation pressure P^{sub}. The solid volume in the exponential term (Poynting correction) is represented by V^S.

An alternative way to calculate the fugacity of the pure solid solute is from the equilibrium condition with a sub-cooled hypothetic liquid. Prausnitz et al. [47] showed that the fugacity of the pure solid solute f^S at temperature T and triple point pressure P_0 is calculated by the following equation:

$$\ln f_i^S(T,P_0) = \ln f_i^L(T,P_0) - \frac{\Delta H_{f,i}}{R}\left(\frac{1}{T}-\frac{1}{T_{f,i}}\right) \tag{2}$$

where $T_{f,i}$ and $\Delta H_{f,i}$ are, respectively, the solute temperature and enthalpy of fusion and where $f_i^L(T,P_0)$ is the solute fugacity in the sub-cooled liquid state.

Including the Poynting corrections to take account of the pressure effect on the solid and liquid fugacities, Eq. (2) holds:

$$\ln f_i^S(T,P) = \ln f_i^L(T,P) + \frac{(V_i^S-V_i^L)}{RT}(P-P_0) - \frac{\Delta H_{f,i}}{R}\left(\frac{1}{T}-\frac{1}{T_{f,i}}\right) \tag{3}$$

The difference between the volumes of the solid and liquid phases is very small, so the second term of Eq. (3) can be canceled.

To calculate the solubility of the solid solute *1* in a supercritical solvent (y_1), it is possible to apply Eq. (1), together with the expression of the solute fugacity in the supercritical phase:

$$y_1 = \frac{P_1^{sub}}{P}\frac{\phi_1^V(T,P^{sub})}{\hat{\phi}_1^V(T,P,y_1)}\exp\left[\frac{V_1^S}{RT}\left(P-P_1^{sub}\right)\right] \tag{4}$$

where P_1^{sub}/P represents the ideal solubility considering the fluid phase as an ideal gas and the remaining three factors are grouped into the so-called enhancement factor E. The order of magnitude of E is mainly determined by the fugacity coefficient of the solute $\hat{\phi}_1^V$ in the fluid phase, which is usually very small at near critical solvent conditions. This means that the solute solubility increases several orders of magnitude in this region.

However, the lack of experimental information on solute sublimation pressure limits the use of Eq. (4) in the calculation of solid-fluid equilibrium.

An alternative way is to apply Eq. (3) to calculate the fugacity of the solid solute making it equal to the fugacity of the solute in the fluid phase [46]. Neglecting the Poynting term of Eq. (3), the solubility of the solute in the supercritical solvent can be calculated as:

$$y_1 = \frac{\phi_1^L(T,P)\times\exp\left[\frac{\Delta H_{f,1}}{R}\left(\frac{1}{T}-\frac{1}{T_{f,1}}\right)\right]}{\hat{\phi}_1^V(T,P,y_1)} \tag{5}$$

The application of Eq. (5) requires information on the temperature and enthalpy of fusion of the solute and the calculation (with an equation of state) of the fugacity coefficient of the pure solute as a hypothetical liquid ϕ_1^L and its fugacity coefficient in the supercritical phase $\hat{\phi}_1^V$.

Eq. (5) is also applicable to calculate the solid-liquid solubility of solute *1*. In this case, the denominator of the equation contains the solute fugacity coefficient in the liquid phase (dependent on temperature, pressure and phase composition). The relation

$$\frac{\hat{\phi}_i^L(T,P,x_i)}{\phi_i^L(T,P)} = \gamma_i \tag{6}$$

represents the activity coefficient of component i in the liquid phase. From Eq. (6), it becomes apparent the possibility of applying an excess energy model G^E to calculate the solubility of a solid solute i in the liquid phase, through an equation equivalent to Eq. (5):

$$x_i = \frac{\exp\left[\frac{\Delta H_{f,i}}{R}\left(\frac{1}{T}-\frac{1}{T_{f,i}}\right)\right]}{\gamma_i}. \tag{7}$$

3. Results and discussion

3.1. Experimental measurements

The solubilities of quinizarin in H_2O were measured at temperatures of (333, 353, 373, 393, 413 and 443) K, and pressures of (30, 60 and 90) bar. The experimental solubilities of quinizarin, in mole fraction (y) and mg/ml (s), are summarized in Table 1 together with the corresponding standard deviations. Each reported solubility is the average value of three replicate samples.

Examination of the solubility data in Table 2 and Fig. 3 reveals that the solubility of the solute increases with increasing temperature at constant pressure, as expected, due to the decrease in water intermolecular interactions (dipole–dipole and hydrogen bonding) at high temperatures [23,26]. Consequently, the dielectric constant of water decreases significantly upon heating and its polarity is reduced, compared to room temperature, favoring the extraction of quinizarin. Also, the solubility increases as the temperature approaches the fusion temperature of quinizarin.

In addition, Table 2 shows that the variation of pressure very slightly affects the solubility of this AQ when the pressure is increased from 30 to 90 bar. This is expected, because liquids are nearly incompressible in the subcritical region; therefore the change in solvating power that accompanies density variation is several orders of magnitude lower, compared to the effect of temperature [23]. In general and in a more clear way for higher temperatures, the increase in pressure seems to promote a decrease in solubility. In general, a solid is less soluble in a given liquid solution

Table 2
Experimental solubilities of quinizarin in mole fractions (y)x10^6 and mg/mL(s) with their corresponding standard deviations (SD).

Temperature (K)	*($y \pm SD$) x10^6*	*$s \pm SD$ (mg/ml)*
30 bar		
333	1.038 ± 0.09	0.0136 ± 0.001
353	1.553 ± 0.03	0.0198 ± 0.001
373	1.977 ± 0.05	0.0253 ± 0.001
393	2.102 ± 0.08	0.0264 ± 0.001
413	3.151 ± 0.03	0.0389 ± 0.001
443	17.03 ± 1.20	0.2040 ± 0.014
60 bar		
333	1.135 ± 0.67	0.0149 ± 0.009
353	1.294 ± 0.85	0.0168 ± 0.011
373	1.551 ± 0.05	0.0198 ±0.001
393	1.716 ± 0.05	0.0219 ± 0.001
413	2.822 ± 0.01	0.0349 ± 0.001
443	13.20 ± 1.20	0.1585 ± 0.015
90 bar		
333	0.937 ± 0.18	0.0123 ± 0.002
353	1.089 ± 0.05	0.0139 ± 0.001
373	1.109 ± 0.02	0.0142 ± 0.001
393	1.209 ± 0.01	0.0152 ± 0.001
413	2.741 ± 0.19	0.0340 ± 0.002
443	10.04 ± 1.40	0.1207 ± 0.017

The uncertainty of the variables are: u(T) = 0.5 K; u(P) = 1 bar; u(y) = 1×10^{-6}, u(s) = 0.005 mg/ml and the combined expanded uncertainty with level of confidence 0.95 (k = 2) for the solubility is: Uc(s) = 0.009mg/ml.

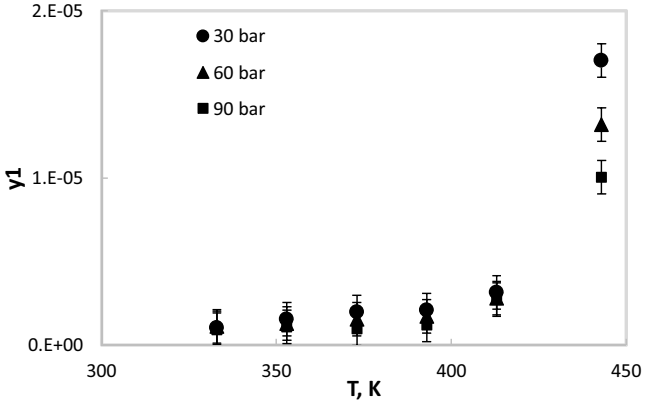

Fig. 3. Experimental solubilities of quinizarin.

under high pressure than under low pressure [48]. This effect can be explained by the volume changes during solubilization [48].

3.2. Model parameterization

In order to model the experimental data a new functional group, called "cyclic ketone" (CyC=O) was defined. The ketone groups in AQs are regarded as cyclic ketones because, although rings 1 and 3 are aromatic, the middle ring has no aromaticity, and therefore can be regarded as an aliphatic cyclic ring [49,50]. Fig. 1 shows the chemical structure of the cyclic ketones compounds studied in this work.

The cyclic ketone group is an associative group with a single electron-donor site. The association in CyC=O only takes place through its electronegative site, capable of cross-associating with electropositive sites of other associative groups.

To include the new CyC=O group in the GCA-EOS model, pure group, binary interaction and association parameters were obtained by regression of experimental equilibrium data of pure compounds and binary systems. The new parameters, as well as the remaining parameters used in this work, are reported in Table 3. A

Table 3
GCA-EoS parameters used to model the cyclic ketones mixtures studied in this work.

Pure group parameters

group	T_i^* (K)	q	g*	gí	g"
CyC=O[a]	600.00	0.640[b]	888410.0	−0.7018	0.0000
AC[a]	600.00	0.285	723210.0	−0.6060	0.0000
ACH[a]	600.00	0.400	723210.0	−0.6060	0.0000
$CyCH_2$[a]	600.00	0.540	466550.0	−0.6062	0.0000
ACOH[c]	600.00	0.680	852819.0	−0.0011	0.2685
H_2O[d]	647.13	0.866	964719.8	−1.2379	1.0084

Binary interaction parameters

group i	group j	k_{ij}	k'_{ij}	α_{ij}	α_{ji}
CyC=O	AC/ACH[a]	0.9250	0.0000	15.000	4.5810
	$CyCH_2$[a]	0.8700	0.0970	5.146	0.8544
	H_2O[b]	0.8900	−0.0990	4.900	9.5000
	ACOH[b]	1.0400	−0.0120	3.800	4.2000
ACOH	AC/ACH[c]	0.8330	0.0000	0.000	0.0000
	$CyCH_2$[a]	0.8930	0.000	0.0000	
	H_2O[c]	1.1002	0.0855	−22.50	2.7700
H_2O	ACH∼[e]	0.9100	−0.0560	2.000	4.0000

Association parameters

		-C/k (K)	κ (cm^3/mol)
Cross-association	CyCO/ACOH[b]	3402	0.8000
	CyCO/H_2O[b]	1550	0.6000
	ACOH/H_2O[c]	2585	0.6335
	ACOH/AR[c]	2200	1.0169
	H_2O/AR[e]	1760	0.2300
Self- association	ACOH/ACOH[c]	2759	0.8709
	H_2O/H_2O[d]	2060	0.3787

a)Skjold-Jørgensen [33]; b) This work; c) Sanchez et al. [45]; d) Soria et al. [42]; e) Sánchez et al. [43].

Table 4
Experimental systems used to test GCA-EoS predictions using the CyC=O functional group.

Systems	*T range* (K)	*P range* (bar)	N^{set}	N^{exp}	*ARD%*	*ADD%*	Ref.
Vapor Pressure							
Cyclohexanone	250-500	1.41×10^{-4}–4.76	1	26	7.05	8.16	[52]
9,10-anthraquinone	559-623	0.12–1.00	1	20	5.75	3.12	[52]
Vapor Liquid Equilibria							
Cyclohexane + cyclohexanone	323-348	0.10–0.82	2	13	5.54	1.20	[53]
Cyclohexanone + toluene	384-427	1.01	1	10	5.58	4.27	[54]

N^{set}: Number of experimental sets, N^{exp}: Number of experimental data.

brief explanation of the parametrization strategy used in this work will be given below.

The pure group parameters for the CyC=O group were set equal to the parameters of the acyclic ketone group defined in the original GC-EOS model. Only the *q* parameter (number of surface segments) was corrected. For the compounds studied in this work, the CyC=O group does not correspond to the original ketone groups ($CH_3C{=}O$ and $CH_2C{=}O$), since it is attached to aromatic carbon atoms, as shown in Fig. 1. For this reason, the (CyC=O) surface parameter q was calculated from van der Waals surface area, according to Bondi [51].

To evaluate the performance of the original ketone group parameters in the description of cyclic ketones, its predictive capability was analyzed by calculating binary vapor liquid equilibria in systems containing cyclohexanone and vapor pressure of 9,10-anthraquinone. Table 4 summarizes the systems studied, the range of conditions, the references and the deviations from the experimental data. As Fig. 4 shows, a good prediction was achieved, confirming that the original parameters of the ketone group (with the corrected value of *q*) can be used with confidence to represent cyclic ketones.

Binary phase equilibrium data were used to obtain the binary interaction and cross-association parameters of the new CyC=O ketone group with water (H_2O) and with phenol (ACOH). The systems included in the correlation are given in Table 5, along with the temperature and pressure range covered, the reference to the experimental data, the number of data sets (N^{set}) and data points (N^{exp}), the average relative deviations (ARD) and the average absolut deviations (AAD) calculated by Eqs. 8 and 9.

$$ARD = 100x \sum \frac{\left(y_s^{exp} - y_s^{calc}\right)/y_s^{exp}}{N} \tag{8}$$

$$AAD = 100x \sum \frac{|y_s^{exp} - y_s^{cal}|}{N} \tag{9}$$

Association effects in phenol were accounted by the electronegative and electropositive sites of the hydroxyl group and by an electronegative site in the aromatic ring [43,45]. Water was considered to have two hydrogen bonding groups with two associating sites each (one electronegative O and one electropositive H), which is equivalent to a 4C association model [42]. The corresponding correlation results are shown in Figs. 5 and 6.

Having obtained the interaction parameters between the CyC=O and the ACOH and H_2O functional groups, the GCA-EOS model was

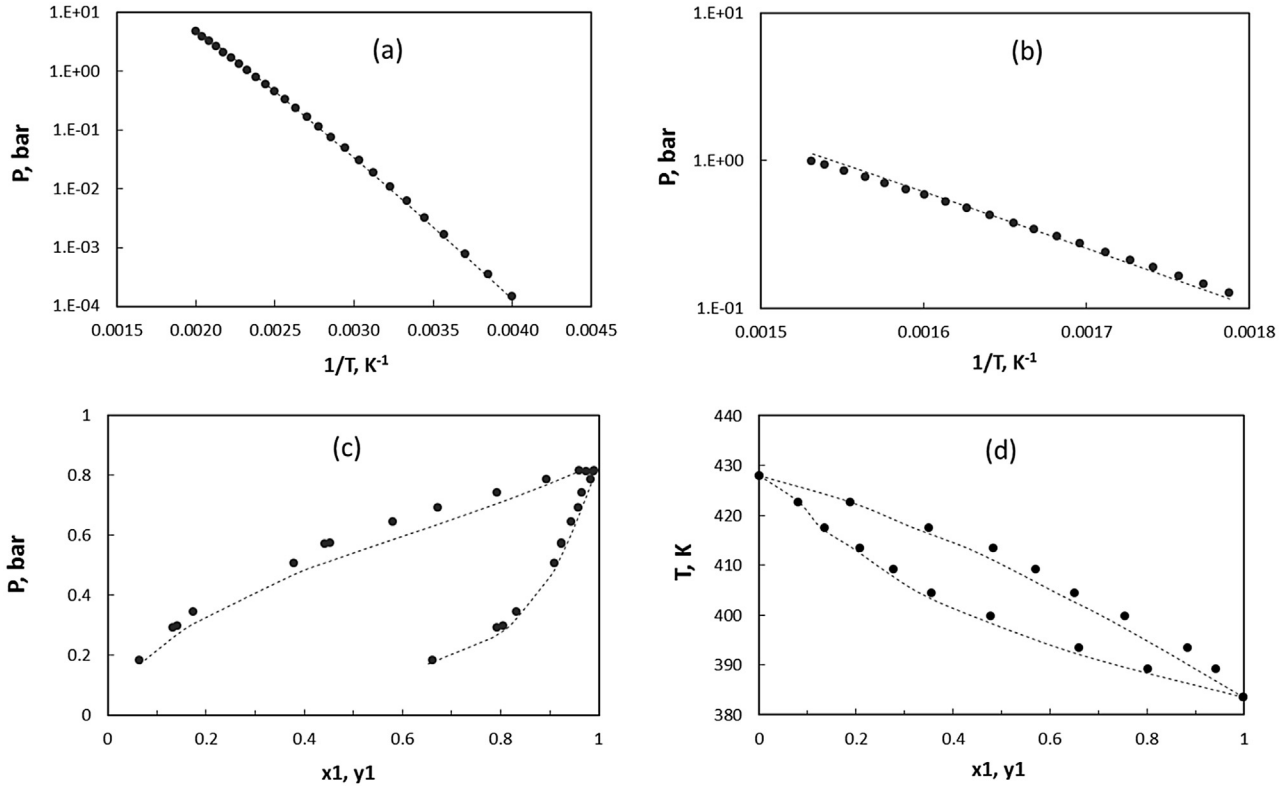

Fig. 4. Comparison between GCA-EOS predictions (dashed lines) and experimental (dots) vapor pressure of (a) cyclohexanone [52]; (b) 9,10-anthraquinone [52], and vapor-liquid equilibria of: (c) cyclohexanone(1) + cyclohexane(2) at T = 348 K [53]; (d) cyclohexanone(1) + toluene(2) at P = 1.013 bar [54].

Table 5
Vapor liquid equilibria experimental data sets used in the correlation process.

Binarysystems	*T range* (K)	*P range* (bar)	N^{set}	N^{exp}	*ARD*	*ADD*	Ref.
Cyclohexanone + phenol	424–458	1.013	1	24	6.89	2.520	[55]
Cyclohexanone + H_2O	273–364	1.013	1	10	18.10	0.005	[56]
Cyclopentanone + H_2O	273–364	1.013	1	10	20.40	1.470	[56]

Table 6
Physical properties of pure cyclic ketones employed in the solid–fluid equilibrium calculations.

Compound	T_c (K)	P_c (bar)	T_b (K)	T_f (K)	ΔH_f ($Jmol^{-1}$)	d_{ci}[e]
9,10-anthraquinone	900.00[b]	31.15[b]	653.05[b]	558.00[a]	32620[a]	5.8100
Anthrone	923.03[c]	32.64[c]	657.50[c]	428.15[a]	26800[a]	5.2500
9,10-phenanthrenequinone	900.00[b]	31.15[b]	653.05[b]	558.00[a]	32620[a]	5.3600
1,4-dihydroxy-9,10-anthraquinone	927.55[c]	48.86[c]	703.00[a]	472.00[a]	19779[d]	5.1280
1,5-dihydroxy-9,10-anthraquinone	927.55[c]	48.86[c]	703.00[a]	472.00[a]	19779[d]	7.7728
1,8-dihydroxy-9,10-anthraquinone	927.55[c]	48.86[c]	703.00[a]	472.00[a]	19779[d]	6.9481
1,2-dihydroxy-9,10-anthraquinone	927.55[c]	48.86[c]	703.00[a]	472.00[a]	19779[d]	5.1280

(a) From NIST (National Institute of Standars-USA) http://webbook.nist.gov/chemistry [57]. (b) From DIPPR801 Database [52]. (c) Calculated with Joback's group contribution method from Poling et al. [58]. (d) Calculated by eq. (8) from Fornari et al. [59]. (e)Calculated by an optimization procedure.

Table 7
Experimental data sets used to check the predictive capacity of the GCA-EoS equation.

Systems	*T range*(K)	*P range*(bar)	N^{set}	N^{exp}	*ARD%*	*ADD%*	Ref.
Vapor Pressure							
1,5-dihydroxy-9,10-anthraquinone	410-510	2.310^{-6}–1.310^{-3}	1	28	13.81	0.005	[60]
1,8-dihydroxy-9,10-anthraquinone	373-456	8.210^{-7}–7.410^{-4}	1	28	14.24	0.002	[60]
Solid Liquid Equilibria							
9,10-anthraquinone + H_2O	313-433	50	1	7	21.17	9.810^{-5}	[28]
Anthrone + H_2O	313-423	50	1	7	11.28	6.810^{-5}	[28]
9,10-phenanthrenequinone + H_2O	313-473	50	1	9	22.32	1.510^{-3}	[28]
1,2-dihydroxy-9,10-anthraquinone + H_2O	398-473	40	1	7	80.12	2.410^{-3}	[26]
1,4-dihydroxy-9,10-anthraquinone + H_2O	333-463	30, 60, 90	3	7	61.00	5.510^{-4}	This work

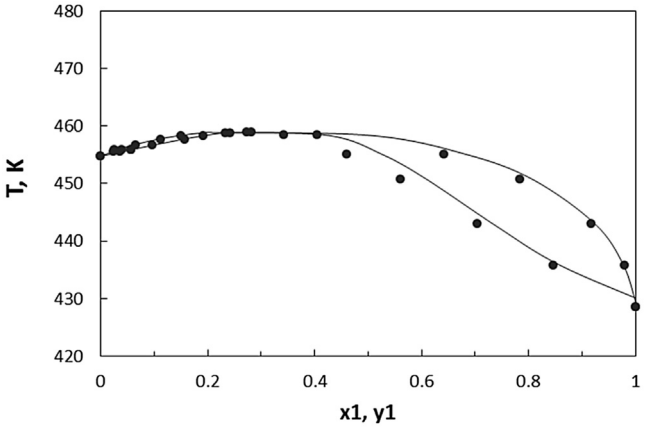

Fig. 5. Comparison between GCA-EOS correlations (solid lines) and experimental data (dots) for vapor-liquid equilibria of cyclohexanone(1) + phenol(2) at P = 1.013 bar[55].

then applied to calculate the solid-fluid equilibria of (AQs + water) binary systems, including the solubility data of quinizarin measured in this work.

Table 6 reports the physical properties (T_c, P_c, T_b, T_f, ΔH_f and d_c) of AQs employed in the calculations. Whenever available, experimental data were used. However, as most of these compounds suffer thermal decomposition before reaching its critical point, their critical properties were calculated by group contribution methods [58,59].

The critical hard-sphere diameter (d_{ci}) of the AQs studied in this work, cannot be calculated following the procedure proposed by Skjold-Jørgensen [34] (i.e., from the values of the critical properties or by fitting experimental vapor pressure data) due to the mentioned uncertainties in the values of the critical properties and also due to their very low volatility. For this reason, the d_{ci} values of AQs were considered adjustable parameters.

Table 7 summarizes the data base used to check the predictive capacity of the GCA-EOS model and reports the absolute and relative deviations between predictions and experimental data. Fig. 7 compares GCA-EOS predictions with experimental vapor pressure data of 1,5-dihydroxy-9,10-anthrquinone and 1,8-dihydroxy-9,10-anthrquinone [60]. It can be observed that in both cases a good agreement was obtained. Fig. 8, on the other side, shows the solubilities of AQs in H_2O. The deviations between experimental [28] and calculated results are very low for 9,10-anthraquinone, anthrone and 9,10-phenanthrenequinone solubility in pressurized hot water, indicating a good capacity of the GCA-EOS model to predict the solubility behavior of these compounds at high pressure conditions. However, deviations from experimental data [26] are important in the case of 1,2-dihydroxy-9,10-anthraquinone. This discrepancy could be attributed to the incapacity of the model to represent the more complex structure of this ketone, which has two different functional groups in the molecule. Fig. 8(e), on the other hand, shows a reasonable agreement between the GCA-EOS predictions and the experimental data of quinizarin measured in this work. More experimental data on the solubility of hydroxy ketones would be necessary to elucidate this point.

The overall performance is satisfactory and the GCA-EOS equation has the potential to model such systems.

4. Conclusions

Multifunctional cyclic compounds found in natural products are of great of interest for the pharmaceutical industry. Pressurized hot water extraction promises to be a good alternative to obtain these products from natural resources. In order to evaluate the viability

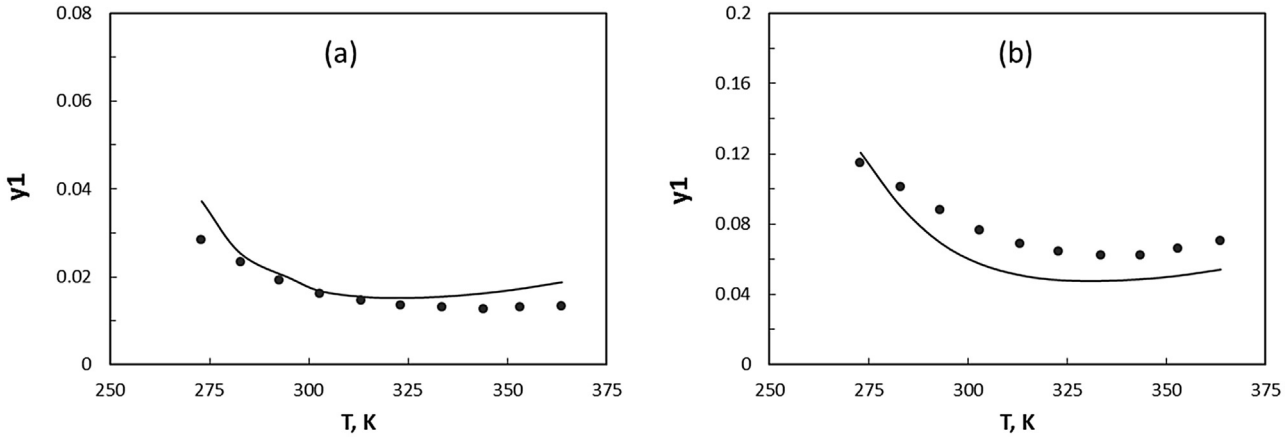

Fig. 6. Comparison between GCA-EOS correlations (solid lines) and experimental data (dots) for liquid–liquid equilibria of: (a) cyclohexanone(1) + H_2O(2)and (b) cyclopentanone(1) + H_2O(2) at P = 1.013 bar[56].

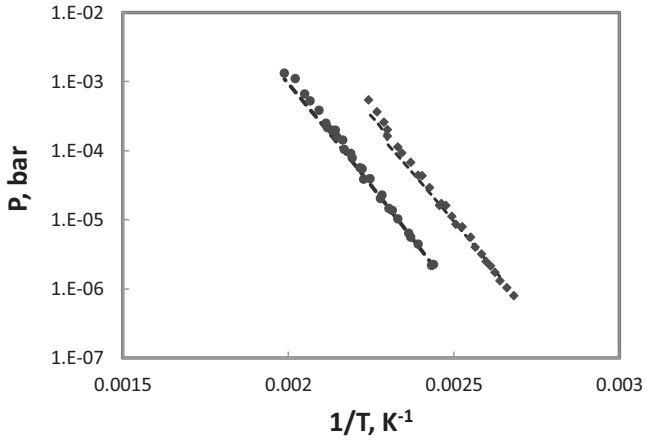

Fig. 7. Comparison between GCA-EOS predictions (dashed lines) and experimental (dots) vapor pressure of: 1,5 dihydroxy-9,10-anthraquinone (●) [60]; (b) 1,8 dihydroxy-9,10-anthraquinone(⧫) [60].

of this process, reliable thermodynamic models are required to predict the phase behaviour of complex mixtures containing water and multifunctional compounds, at high temperatures and pressures.

In this work, the solubility of quinizarin in pressurized hot water at different pressures and temperatures was measured. The solubility increases with the temperature, from 1.038×10^{-6} (333 K) to 17.026×10^{-6}(443 K) at 30 bar, from 1.135×10^{-6} (333 K) to 13.199×10^{-6} (443 K) at 60 bar and from 0.937×10^{-6} (333 K) to 10.038×10^{-6} (443 K) at 90 bar. The parameters of the group-contribution GCA-EOS model were extended to include cyclic ketones. For this purpose, a new cyclic ketone (CyC=O) functional group was defined, and the corresponding parameters were determined. These parameters provided a satisfactory representation of the vapor pressure and solid-liquid equilibria of AQs + H_2O systems. The overall performance is satisfactory and we can conclude that the GCA-EOS equation has the potential to model such systems.

Acknowledgments

The authors acknowledge financial support from the National Research Council of Argentina (PIP 2015-2017), Universidad Nacional del Sur (UNS), Universidad Nacional de Córdoba (Res. 203/14) and Universidad Tecnológica Nacional (PID 3486 and PID 3458).

Appendix A.

GCA-EOS Equation

There are three contributions to the residual Helmholtz energy in the GCA-EOS model: free volume (A^{fv}), attractive (A^{att}) and associative (A^{assoc}). The free volume and attractive contributions are based on Carnahan-Starling and NRTL models respectively, and keep the same form as the original GC-EOS Skjøld-Jorgensen equation [33,34].

$$A^{res} = A^{fv} + A^{att} + A^{assoc} \quad (A.1)$$

The free volume contribution is represented by the extended Carnahan-Starling equation for mixtures of hard spheres developed by Mansoori and Leland [61]:

$$(A/RT)^{fv} = 3\left(\frac{\lambda_1\lambda_2}{\lambda_3}\right)(\text{Y-1}) + \left(\frac{\lambda_2^3}{\lambda_3^2}\right)(-Y + Y^2 - \ln Y) + n\ln Y \quad (A.2)$$

with:

$$Y = \left(1\text{-}\frac{\pi\lambda_3}{6V}\right)^{-1} \quad (A.3)$$

and

$$\lambda_k = \sum_i^{NC} n_i d_i^k \quad (A.4)$$

n_i being the number of moles of component i, NC the number of components in the mixture, n the total number of moles, V the total volume and d_i the hard-sphere diameter per mol of species i.

The following generalized expression gives the temperature dependence of the hard-sphere diameter:

$$d_i = 1.065655 d_{ci}\left[1 - 0.12\exp\left(-\frac{2T_{ci}}{3T}\right)\right] \quad (A.5)$$

where d_{ci} and T_{ci} are, respectively, the critical hard-sphere diameter and critical temperature of component i.

There are three different ways to calculate d_c of each component: *(i)* direct calculation with the values of critical temperature and pressure so that the model fulfills the critical point and its conditions (first and second derivatives of pressure with regard to volume equal to zero) [33], *(ii)* fit d_c to an experimental pure component vapor pressure data point (T^{sat}, P^{sat}) [33], and *(iii)* computation with the correlation proposed by Bottini et al. [62] for high molecular weight compounds.

In the case of permanent gases and molecular compounds, the first procedure must be used. For ordinary solvents method *(ii)*

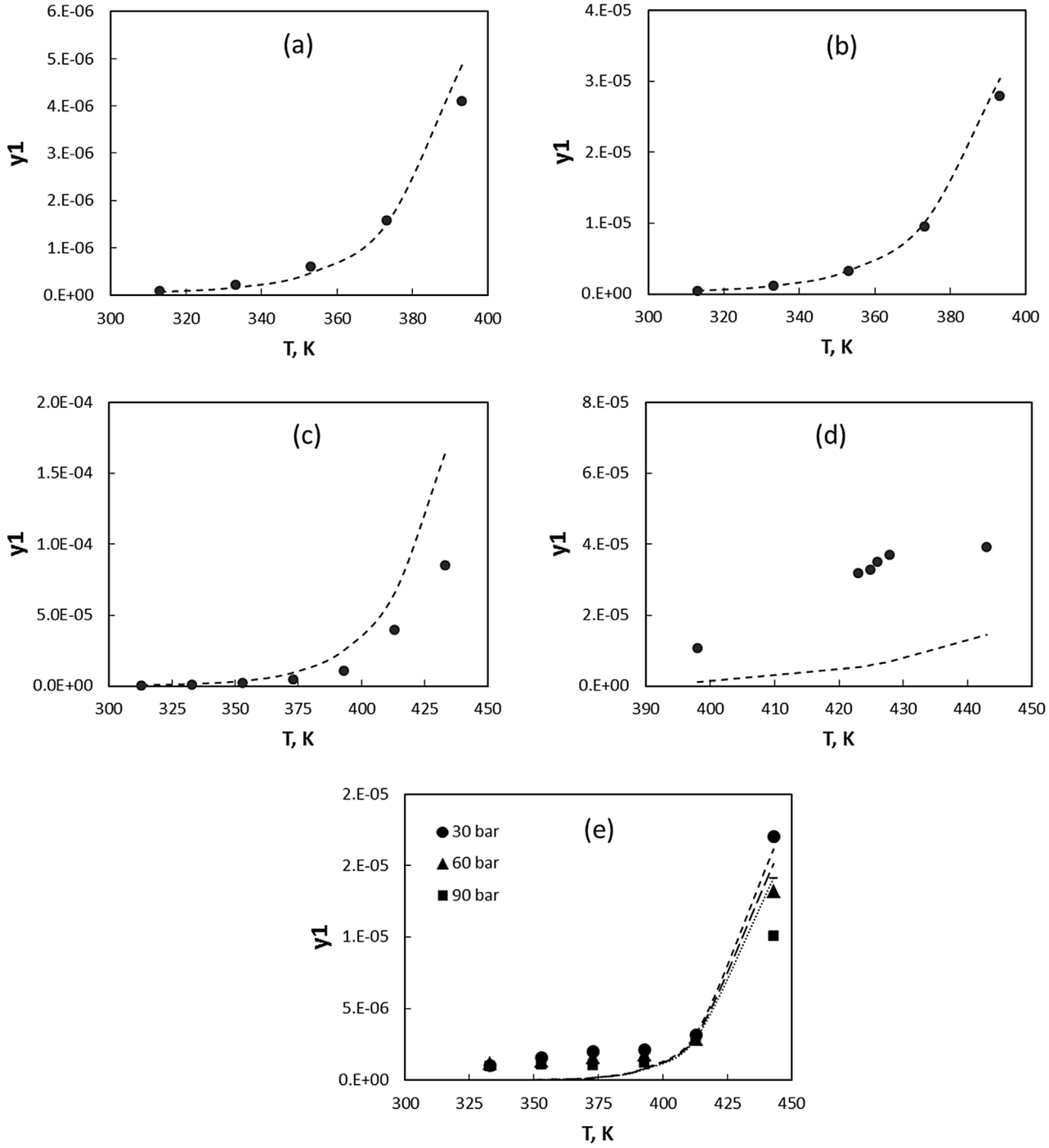

Fig. 8. Comparison between GCA-EOS predictions (dashed lines) and experimental (dots) solubility of different AQs in pressurized water: (a) 9,10-anthraquinone[28]; (b) anthrone[28]; (c) 9,10-phenanthronequinone[28]; (d) 1,2-dihydroxy-9,10-anthraquinone [26]; (e) quinizarin at 30 bar (●), 60 bar (▲) and 90 bar (■).

is generally applied; the d_c values obtained by this way are usually within 5% of the d_c given by method *(i)*, but this difference is significant since pure component vapor pressures are sensitive to d_c[33]. Even more sensitive to the d_c value are the predictions of liquid–liquid equilibria. In this case, better results are achieved when d_c is closer to the value calculated with the critical point conditions (method *i*).

The attractive contribution to the Helmholtz energy accounts for dispersive forces between functional groups, through a density-dependent, local-composition expression based on the NRTL model [63]:

$$(A/RT)^{att} = -\frac{z}{2}\sum_{i}^{NC} n_i \sum_{j}^{NG} v_j^i q_j \sum_{k}^{NG} (\theta_k g_{kj} \tilde{q} \tau_{kj}/RTV) / \sum_{l}^{NG} \theta_l \tau_{lj} \qquad (A.6)$$

with:

$$\tilde{q} = \sum_{i}^{NC} n_i \sum_{j}^{NG} v_j^i q_j \qquad (A.7)$$

$$\theta_j = \left(\frac{q_j}{\tilde{q}}\right)\sum_{i}^{NC} n_i \nu_j^i \tag{A.8}$$

$$\tau_{ij} = \exp\left(\frac{\alpha_{ij}\Delta g_{ij}\tilde{q}}{RTV}\right) \tag{A.9}$$

$$\Delta g_{ij} = g_{ij} - g_{jj} \tag{A.10}$$

z being the coordination number (set equal to 10), ν_j^i the number of groups of type j in molecule i, q_j the number of surface segments assigned to group j, $\tilde{q}$ the total number of surface segments, θ_k the surface fraction of group k, g_{ij} the attractive energy between segments of groups i and j, and α_{ij} the non-randomness parameter.

The attractive energy g_{ij} is calculated from the energy between like-group segments trough the following combination rule:

$$g_{ij} = k_{ij}(g_{ii}g_{jj})^{1/2} \tag{A.11}$$

where the binary interaction parameter k_{ij} is symmetrical ($k_{ij} = k_{ji}$). Both, the attractive energy between like segments and the binary interaction parameter are temperature dependent:

$$g_{jj} = g_{jj}^{*}\left[1 + g_{jj}^{'}\left(\frac{T}{T_j^{*}} - 1\right) + g_{jj}^{''}\ln\left(\frac{T}{T_j^{*}}\right)\right] \tag{A.13}$$

$$k_{ij} = k_{ij}^{*}\left[1 + k_{ij}^{'}\ln\left(\frac{2T}{(T_i^{*} + T_j^{*})}\right)\right] \tag{A.14}$$

where T_i^{*} is an arbitrary but fixed reference temperature for group i; g_{jj}^{*}, $g_{jj}^{'}$ and $g_{jj}^{''}$ are pure-group energy parameters and k_{ij}^{*} and $k_{ij}^{'}$ are binary group interaction parameters.

The association contribution to the Helmholtz function is calculated with a group contribution expression [34,37[]] based on Whertheim's theory [64] of associating fluids:

$$\frac{A^{assoc}}{RT} = \sum_{i=1}^{NGA} n_i^{assoc}\left[\sum_{k=1}^{M_i}\left(\ln X^{(k,i)} - \frac{X^{(k,i)}}{2}\right) + \frac{1}{2}M_i\right] \tag{A.15}$$

where NGA represents the number of associating groups, n_i^{assoc} the number of moles of associating group i, M_i the number of associating sites assigned to group i and $X^{(k,i)}$the mole fraction of group i not bonded at site k. The number of moles of associating group i is:

$$n_i^{assoc} = \sum_{m=1}^{NC} \nu_m^{i,assoc} n_m \tag{A.16}$$

where $\nu_m^{i,assoc}$ represents the number of associating group i is present in molecule m and n_m is the total amount of moles of species m; the summation includes all NC components in the mixture.

The mole fraction of group i not bonded at site k is determined from the following expression:

$$X^{(k,i)} = \left[1 + \sum_{j=1}^{NGA}\sum_{l=1}^{M_j}\rho_j^{assoc} X^{(l,j)}\Delta^{(k,i,l,j)}\right]^{-1} \tag{A.17}$$

where the summation includes all NGA associating groups and M_j sites. $X^{k,i}$ depends on the molar density of the associating group and on the association strength $\Delta^{k,i,l,j}$.

$$\rho_j^{*} = \frac{n_j^{*}}{V} \tag{A.18}$$

$$\Delta^{k,i,l,j} = \kappa^{k,i,l,j}[\exp(\epsilon^{k,i,l,j}/kT) - 1] \tag{A.19}$$

The association strength between site k of group i and site l of group j depends on the temperature T and on the association parameters κ and ε, which represent the volume and energy of association, respectively.

The thermodynamic properties required to calculate phase equilibria are obtained by differentiating the residual Helmholtz energy. The association contributions to the compressibility factor Z and to the fugacity coefficient &x3D5;$_i$ of component i in the mixture are given by:

$$Z_{\text{assoc}} = -\frac{V}{n}\frac{\partial}{\partial V}((A^R/RT)_{\text{assoc}})_{T,n} = -\frac{V}{n}\sum_{i=1}^{\text{NGA}} n_i^{*}\left[\sum_{k=1}^{M_i}\left(\frac{1}{X^{(k,i)}} - \frac{1}{2}\right)\left(\frac{\partial_X^{(k,i)}}{\partial V}\right)_{T,n}\right] \tag{A.20}$$

$$\ln\phi_q^{\text{assoc}} = \frac{\partial}{\partial n_q}((A^R/RT)_{\text{assoc}})_{T,V,n_{r\neq q}}$$

$$\ln\phi_q^{\text{assoc}} = \sum_{i=1}^{\text{NGA}}\left\{V_{\text{assoc}}^{(i,q)}\left[\sum_{k=1}^{M_i}\left(\ln X^{(k,i)} - \frac{X^{(k,i)}}{2}\right) + \frac{M_i}{2}\right] + n_i^{*}\left[\sum_{k=1}^{M_i}\left(\frac{1}{X^{(k,i)}} - \frac{1}{2}\right)\left(\frac{\partial_X^{(\mathrm{k,i})}}{\partial_{\mathrm{n_q}}}\right)_{\mathrm{T,V},n_{r\neq q}}\right]\right\} \tag{A.21}$$

The final expressions of these contributions depend on the number of associating groups NGA and on the number of associating sites M_i assigned to each group i.

Calculation of association effects is based on the minimization approach proposed by Michelsen and Hendriks[65] and Tan et al. [66], procedure to calculate the fraction of non-associating sites. Detailed of this procedure has been reported by Soria et al. [67].

References

[1] M.M. Cowan, Plant Products as antimicrobial agents, Clin. Microbiol. Rev. 12 (1999) 564–582.

[2] R. Wijnsma, R. Verpoorte, in: W. Herz, H. Grisebach, G.W. Kirby, C. Tamm (Eds.), Prog. Chem. Org. Nat. Prod., vol. 49, Springer-Verlag, Wien, 1986, pp. 79–149.

[3] G. Rath, M. Ndonza, K. Hostettmann, Antifungal anthraquinones from Morinda lucida, Int. J. Pharmacognosym. 33 (1995) 107–114.

[4] A.M. Ali, N.H. Ismail, M.M. Mackeen, L.S. Yazan, S.M. Mohamed, A.S.H. Ho, N.H. Lajis, Antiviral, cytotoxic and antimicrobial activities of anthraquinones isolated from the roots of Morinda elliptica, Pharm. Biol. 38 (2000) 298–301.

[5] S.K. Agarwal, S.S. Singh, S. Verma, S. Kumar, Antifungal activity of anthraquinone derivatives from Rheum emodi, J. Ethnophamacol. 72 (2000) 43–46.

[6] L.R. Comini, S.C. Núñez Montoya, P.L. Paéz, G.A. Argüello, I. Albesa, J.L. Cabrera, Antibacterial activity of anthraquinone derivatives from *Heterophyllaea pustulata* (Rubiaceae), J. Photochem. Photobiol. B 102 (2011) 108–114.

[7] B.S. Konigheim, M. Beranek, L.R. Comini, J.J. Aguilar, J. Marioni, M.S. Contigiani, S.C. Núñez Montoya, In vitro antiviral activity of *Heterophyllaea pustulata* extracts, Nat. Prod. Commun. 7 (2012) 1025–1028.

[8] M.L. Vickery, B. Vickery, Secondary Plant Metabolism; University Park Press, Baltimore. Leistner, E. In: The Biochemistry of Plants –A comprehensive treatise (eds. P.K. Stumpf and E.E. Conn); Academic Press New York.; 7, 403-423 (1981).

[9] G.C.H. Derksen, T.A. Van Beek, A.E. de Groot, A. Capelle, High-performance liquid chromatographic method for the analysis of anthraquinone glycosides and aglycones in madder root (Rubia tinctorum L.), J. Chromatogr. A. 816 (1998) 277–281.

[10] L. Hoi-Seon, Inhibitory effects of quinizarin isolated from cassia tora seeds against human intestinal bacteria and aflatoxin B1 biotransformation, J. Microbiol. Biotechnol. 13 (2003) 529–536.
[11] N.D. Davis, S.K. Iyer, U.L. Diener, Improved method of screening for aflatoxin with a coconut agar medium, Appl. Environ. Microbiol 53 (1987) 1593–1595.
[12] B.Y. Kwak, D.H. Shon, B.J. Kwon, C.-H. Kweon, K.H. Lee, Detection of Aspergillus and Penicillium genera by enzyme-linked immunosorbent assay using a monoclonal antibody, J. Microbiol. Biotechnol. 11 (2001) 22–28.
[13] S.C. Núñez Montoya, A.M. Agnese, C. Pérez, I.N. Tiraboschi, J.L. Cabrera, Pharmacological and toxicological activity of Heterophyllae pustulata anthraquinone extracts, Phytomedicine 105 (2003) 69–574.
[14] S.C. Núñez Montoya, A.M. Agnese, J.L. Cabrera, Anthraquinone derivatives from Heterophyllaea pustulata, J. Nat. Prod. 69 (2006) 801–803.
[15] A.M. Shami, Isolation and identification of anthraquinones extracted from Morinda Citrifolia L. (Rubiaceae), Ann. Chromatogr. Sep. Technol. 1 (2015) 1012–1014.
[16] V. Mohanlall, P. Steenkamp, B. Odhav, Isolation and characterization of anthraquinone derivatives from Ceratotheca triloba(Bernh.) Hook f, J. Med. Plant. Res. 5 (2011) 3132–3141.
[17] L. Ramos, E.M. Kristenson, U.A.T. Brinkman, Current use of pressurised liquid extraction and subcritical water extraction in environmental analysis, J. Chromatogr. A. 975 (2002) 3–29.
[18] A. Mustafa, C. Turner, Pressurized liquid extraction as a green approach in food and herbal plants extraction: a review, Anal. Chim. Acta. 703 (2011) 8–18.
[19] D.J. Miller, S.B. Hawthorne, Solubility of liquid organic flavor and fragrance compounds in subcritical (hot/liquid) water from 298 to 473 K, J. Chem. Eng. Data 45 (2000) 315–318.
[20] A. Basilea, M.M. Jimenez-Carmona, A.A. Clifford, Extraction of rosemary by superheated water, J. Agric. Food Chem. 46 (1998) 5205–5209.
[21] G. Gmiz and M. D. Luque de Castro, Continuous Sub- Critical Water Extraction of Medicinal Plant Essential Oil Comparison with Conventional Techniques, Talanta. 51 (2000) 1179–1185.
[22] M.F. Barrera Vázquez, L.R. Comini, J.M. Milanesio, S.C. Núñez Montoya, J.L. Cabrera, S. Bottini, R.E. Martini, Pressurized hot water extraction of anthraquinones from Heterophyllaea pustulata Hook f. (Rubiaceae), J. Supercrit. Fluids 101 (2015) 170–175.
[23] M.F. Barrera Vázquez, L.R. Comini, R.E. Martini, S.C. Núñez Montoya, S. Bottini, J.L. Cabrera, Comparisons between conventional, ultrasound-assisted and microwave-assisted methods for extraction of anthraquinones from *Heterophyllaea pustulata* Hook f. (Rubiaceae), Ultrason. Sonochem. 21 (2014) 478–484.
[24] A. Shotipruk, J. Kiatsongserm, P. Pavasant, M. Goto, M. Sasaki, Pressurized hot water extraction of anthraquinones from the roots of *Morinda citrifolia*, Biotechnol. Prog. 20 (2004) 1872–1875.
[25] B. Pongnaravane, M. Goto, M. Sasaki, T. Anekpankul, P. Pavasant, A. Shotipruk, Extraction of anthraquinones from roots of *Morinda citrifolia* by pressurized hot water: antioxidant activity of extracts, J. Supercrit. Fluids 37 (2006) 390–396.
[26] T. Anekpankul, M. Goto, M. Sasaki, P. Pavasant, A. Shotipruk, Extraction of anti-cancer damnacanthal from roots of *Morinda citrifolia* by subcritical water, Sep. Purif. Technol. 55 (2007) 343–349.
[27] P. Karásek, J. Planeta, M. Roth, Solubilities of oxygenated aromatic solids in pressurized hot water, J. Chem. Eng. Data. 54 (2009) 1457–1461.
[28] D.J. Miller, A.A. Clifford, Solubility of polycyclic aromatic hydrocarbons in subcritical water from 298 to 498 K, J. Chem. Eng. Data. 43 (1998) 1043–1047.
[29] C.C. Huang, M. Tang, W.H. Tao, Y.P. Chen, Calculation of the solid solubilities in supercritical carbon dioxide using a modified mixing model, Fluid Phase Equilib. 179 (2001) 67–84.
[30] M. Skerget, Z. Novak-Pintaric, Z. Knez, Z. Kravanja, Estimation of solid solubilities in supercritical carbon dioxide: Peng-Robinson adjustable binary parameters in the near critical region, Fluid Phase Equilib. 203 (2002) 111–132.
[31] P. Coutsikos, K. Magoulas, G.M. Kontogeorgis, Prediction of solid-gas equilibria with the Peng-Robinson equation of state, J. Supercrit. Fluids. 25 (2003) 197–212.
[32] H.P. Gros, S. Bottini, E.A. Brignole, A group contribution equation of state for associating mixtures, Fluid Phase Equilib. 116 (1996) 537–544.
[33] S. Skjold-Joergensen, Group contribution equation of state (GC-EOS): a predictive method for phase equilibrium computations over wide ranges of temperature and pressures up to 30 MPa, Ind. Eng. Chem. Res. 27 (1988) 110–118.
[34] S. Skjold-Jørgensen, Gas solubility calculations. II. Application of a new group-contribution equation of state, Fluid Phase Equilib. 16 (1984) 317–351.
[35] S. Espinosa, G.M. Foco, A. Bermúdez, T. Fornari, Revision and extension of the group contribution equation of state to new solvent groups and higher molecular weight alkanes, Fluid Phase Equilib. 172 (2000) 129–143.
[36] S. Espinosa, T. Fornari, S.B. Bottini, E.A. Brignole, Phase equilibria in mixtures of fatty oils and derivatives with near critical fluids using the GC-EOS model, J. Supercrit. Fluids. 23 (2002) 91–102.
[37] H.P. Gros, S.B. Bottini, E.A. Brignole, High pressure phase equilibrium modeling of mixtures containing associating compounds and gases, Fluid Phase Equilib. 139 (1997) 75–87.
[38] O. Ferreira, E.A. Brignole, E.A. Macedo, Modelling of phase equilibria for associating mixtures using an equation of state, J. Chem. Thermodyn. 36 (2004) 1105–1117.
[39] S. Espinosa, S. Díaz, T. Fornari, Extension of the group contribution associating equation of state to mixtures containing phenol, aromatic acid and aromatic ether compounds, Fluid Phase Equilib. 231 (2005) 197–210.
[40] T. Fornari, Revision and summary of the group contribution equation of state parameter table: application to edible oil constituents, Fluid Phase Equilib. 262 (2007) 187–209.
[41] O. Ferreira, E.A. Macedo, E.A. Brignole, Application of the GCA-EOS model to the supercritical processing of fatty oil derivatives, J. Food Eng. 70 (2005) 579–587.
[42] T.M. Soria, F.A. Sanchez, S. Pereda, S.B. Bottini, Modeling alcohol + water + hydrocarbon mixtures with the group contribution with association equation of state GCA-EOS, Fluid Phase Equilib. 296 (2010) 116–124.
[43] F.A. Sanchez, S., Pereda, E.A., Brignole, GCA-EOS. A SAFT group contribution model—Extension to mixtures containing aromatic hydrocarbons and associating compounds, Fluid Phase Equilib. 306 (2011) 112–123.
[44] T.M. Soria, F.A. Sanchez, S. Pereda, S.B. Bottini, Modeling the phase behavior of cyclic compounds in mixtures of water, alcohols and hydrocarbons, Fluid Phase Equilib. 361 (2014) 143–154.
[45] F.A. Sanchez, S., Pereda, E.A. Brignole. GCA-EOS extension to phenols with hydrocarbons and water. IX Iberoamerican Conferenceon Phase Equilibria and Fluid Properties for Process Design (EQUIFASE 2012, Puerto Varas, Chile), 10.13140/2.1.2626.6401.
[46] A.E. Andreatta, Equilibrio entre fases en el procesamiento de productos naturales. Ph.D. Tesis, Universidad Nacional del Sur, Argentine, 2008.
[47] J.M. Prausnitz, R.N., Lichtenthaler, E.G. Azevedo, Molecular thermodynamics of fluid-phase equilibria, Prentice-Hall PTR, 1999.
[48] R.E. Gibson, On the effect of pressure on the solubility of solid in liquids. Amer. Jour. Sci. 5th serie, 35 A (1938) 49–59.
[49] P. Cysewski, Application of aromaticity indices as molecular descriptors for prediction of optical properties of 9,10-anthraquinone derivatives in ethanol solution, J. Theor. Comput. Chem. 12 (2013) 1350050–1350064.
[50] J. Kozísek, M. Breza, L. Ulický, Aromatic character of anthraquinone derivatives, Chem. Papers 47 (1993) 34–37.
[51] A. Bondi, *Physical Properties of Molecular Crystals, Liquids and Gases*. John Wiley and Sons, Inc New York, 1968.
[52] DIPPR801-Database, Thermophysical Properties Database, 1998.
[53] T. Boublik, B.C.Y. Lu, Vapor-liquid equilibria of the cyclohexane + cyclohexanone system at 323.15 and 348.15 K, J. Chem. Eng. Data. 22 (1977) 331–333.
[54] V.A., Kireev, Y.N. Sheinker, E.M. Peresleni, Zh. Fiz. Khim. 26 (1952) 352-357, cited in DECHEMA Data Series.
[55] A. Aarna, T. Kaps., EestiTead.Akad. Toim., Keem. Geol. 23 (1974)16-21 cited in *DECHEMA* Data Series.
[56] R.M. Stephenson, Mutual solubilities: water-ketones, water-ethers, and water-gasoline-alcohols, J. Chem. Eng. Data. 37 (1992) 80–95.
[57] From NIST (National Institute of Standars-USA), http://webbook.nist.gov/chemistry. (accessed 28 December 2016).
[58] B.E. Poling, J.M., Prausnitz, J.P. O' Connell, The properties of gases and liquids. 2001: McGraw-Hill.
[59] T. Fornari, A. Chafer, R.P. Stateva, G. Reglero, A new development in the application of the group contribution associating equation of state to model solid solubilities of phenolic compounds in SC-CO_2, Ind. Eng. Chem. Res. 44 (2005) 8147–8156.
[60] G. Bardi, R. Gigli, L. Malaspina, V. Piacente, Vapor pressure and sublimation enthalpy of anthraquinone and of 1,5- and 1,8-dihydroxyanthraquinones, J.Chem. Eng. Data. 18 (1973) 126–130.
[61] G.A. Mansoori, T.W. Leland Jr., Statistical thermodynamics of mixtures. A new version for the theory of conformal solution, JCS Faraday Trans. 2. 68 (1972) 320–344.
[62] S.B. Bottini, T. Fornari, E.A. Brignole, Phase equilibrium modelling of triglycerides with near critical solvents, Fluid Phase Equilib. 158–160 (1999) 211–218.
[63] H. Renon, J.M. Prausnitz, Local composition in thermodynamics excess functions for liquid mixtures, AIChE J. 14 (1968) 135–144.
[64] M.J. Wertheim, Fluids with highly directional attractive forces. I. Statistical thermodynamics, J. Stat. Phys. 35 (1984) 19–34.
[65] M.L. Michelsen, E.M. Hendriks, Physical properties from association models, Fluid Phase Equilib. 180 (2001) 165–174.
[66] S.P. Tan, H. Adidharma, M. Radosz, Generalized procedure for estimating the fractions of nonbonded associating molecules and their derivatives in thermodynamic perturbation theory, Ind. Eng. Chem. Res. 43 (2003) 203–208.
[67] T.M. Soria, A.E. Andreatta, S. Pereda, S.B. Bottini, Thermodynamic modeling of phase equilibria in biorefineries, Fluid Phase Equilib. 302 (2011) 1–9.